Electronic Supplementary Material (ESI) for Faraday Discussions.


# Properties of aqueous electrolyte solutions at carbon electrodes: effects of concentration and surface charge on solution structure, ion clustering and thermodynamics in the electric double layer

## Supporting Information

Aaron R. Finney and Matteo Salvalaglio

*Thomas Young Centre and Department of Chemical Engineering, University College London, London WC1E 7JE, United Kingdom*

E-mail: a.finney@ucl.ac.uk; m.salvalaglio@ucl.ac.uk

# Additional Figures

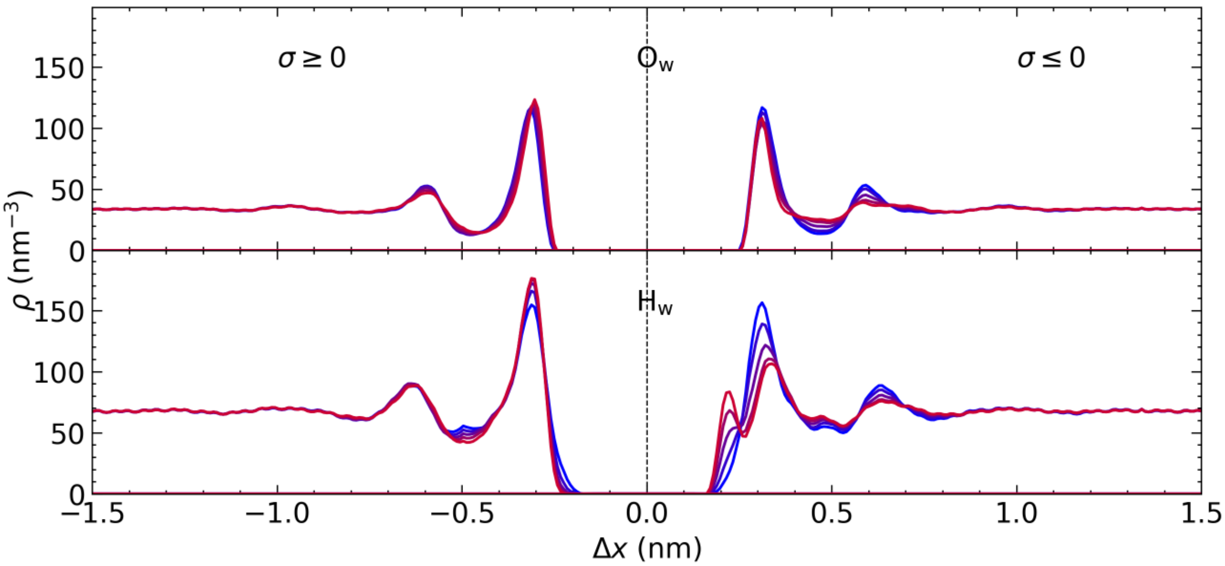


Figure S1: Water atom densities, $\rho$, in the steady state determined as a function of distance from the graphite electrode, $\Delta x$. The atom type is indicated on each panel. Colours blue→red indicate increasing graphite surface charge densities from $|\sigma| = 0 \rightarrow 0.77\ e\ \mathrm{nm}^{-2}$, with data on the left and right of each panel pertaining to simulations with positive and negative applied surface charges, respectively.

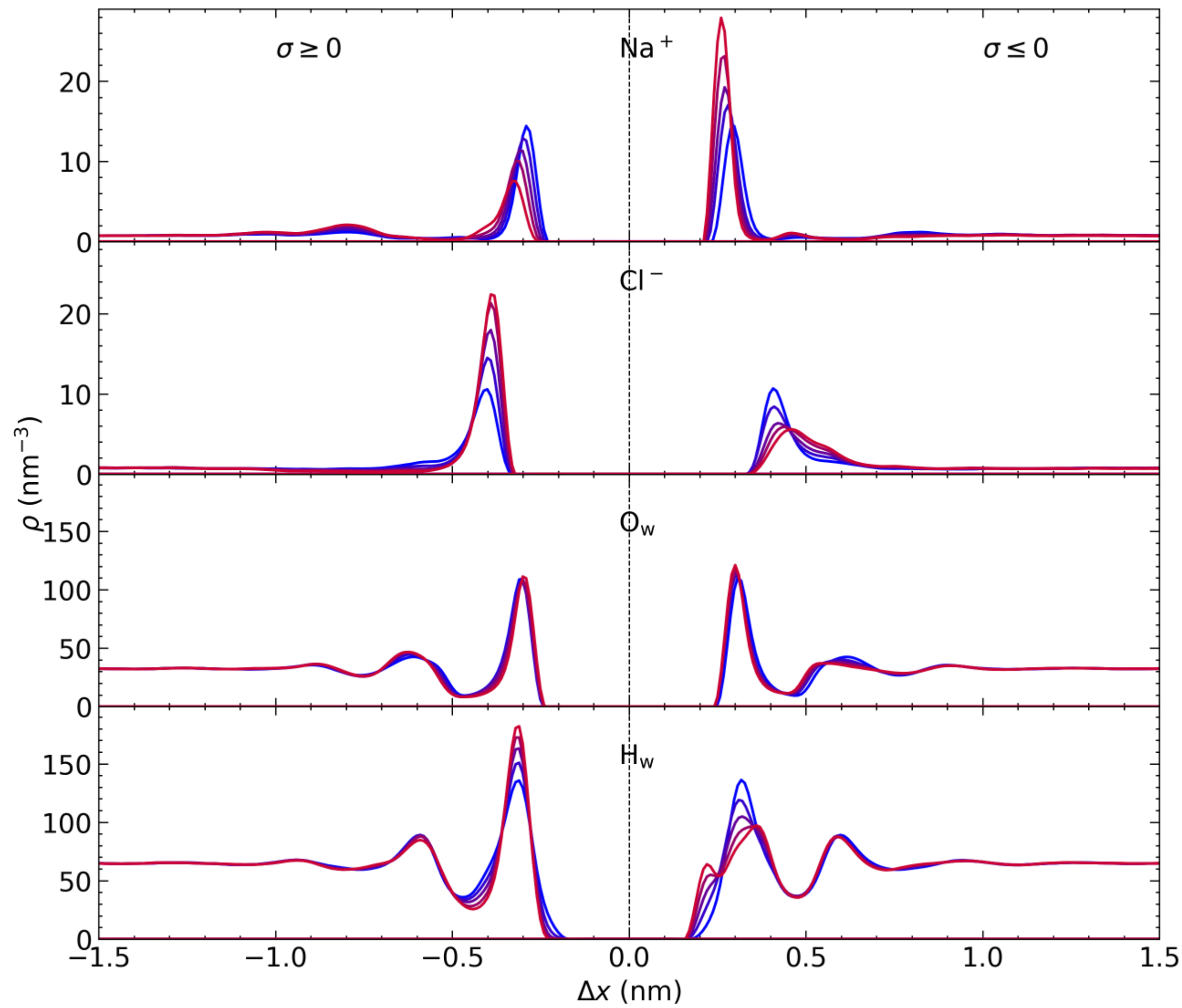


Figure S2: Water atom and ion solution densities, $\rho$, in the steady state determined as a function of distance from the graphite electrode, $\Delta x$, where the target bulk ion concentration was 1 M. The atom type is indicated on each panel. Colours blue→red indicate increasing graphite surface charge densities from $|\sigma| = 0 \rightarrow 0.77\ e\ \mathrm{nm}^{-2}$, with data on the left and right of each panel pertaining to simulations with positive and negative applied surface charges, respectively.

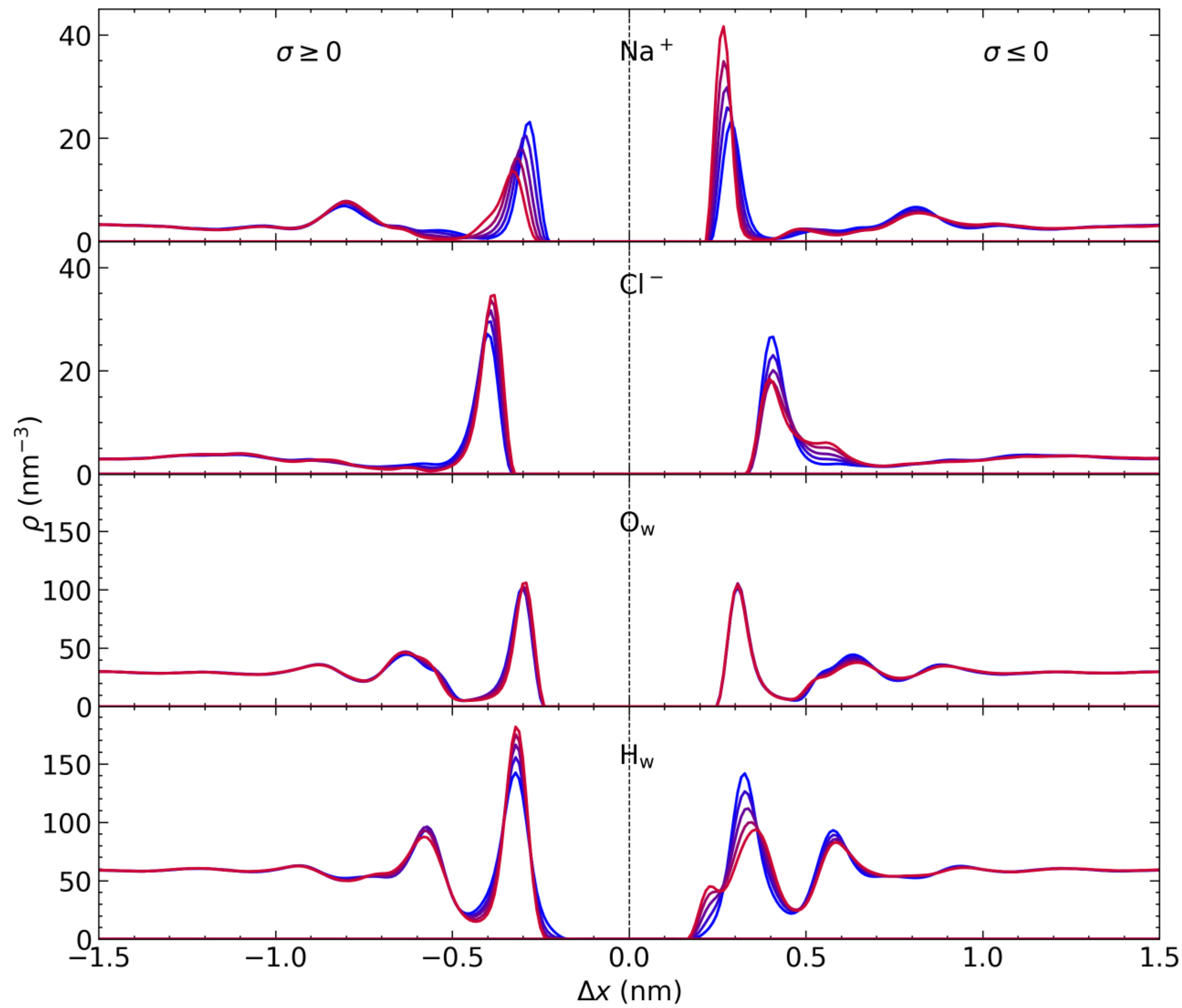


Figure S3: Water atom and ion solution densities, $\rho$, in the steady state determined as a function of distance from the graphite electrode, $\Delta x$, where the target bulk ion concentration was 5 M. The atom type is indicated on each panel. Colours blue→red indicate increasing graphite surface charge densities from $|\sigma| = 0 \rightarrow 0.77\ e\ \mathrm{nm}^{-2}$, with data on the left and right of each panel pertaining to simulations with positive and negative applied surface charges, respectively.

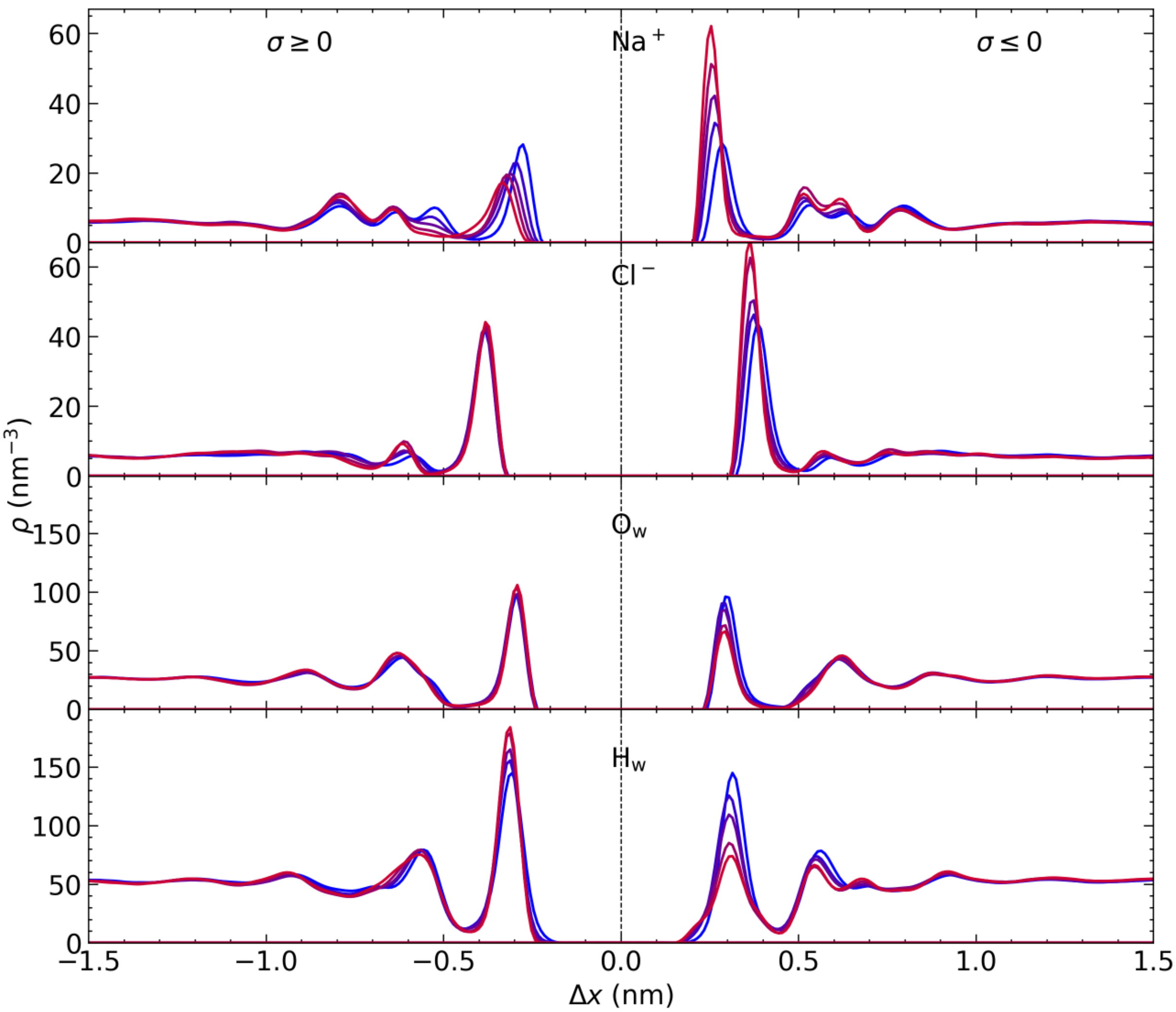


Figure S4: Water atom and ion solution densities, $\rho$, in the steady state determined as a function of distance from the graphite electrode, $\Delta x$, where the target bulk ion concentration was 10 M. The atom type is indicated on each panel. Colours blue→red indicate increasing graphite surface charge densities from $|\sigma| = 0 \rightarrow 0.77\ e\ \mathrm{nm}^{-2}$, with data on the left and right of each panel pertaining to simulations with positive and negative applied surface charges, respectively.

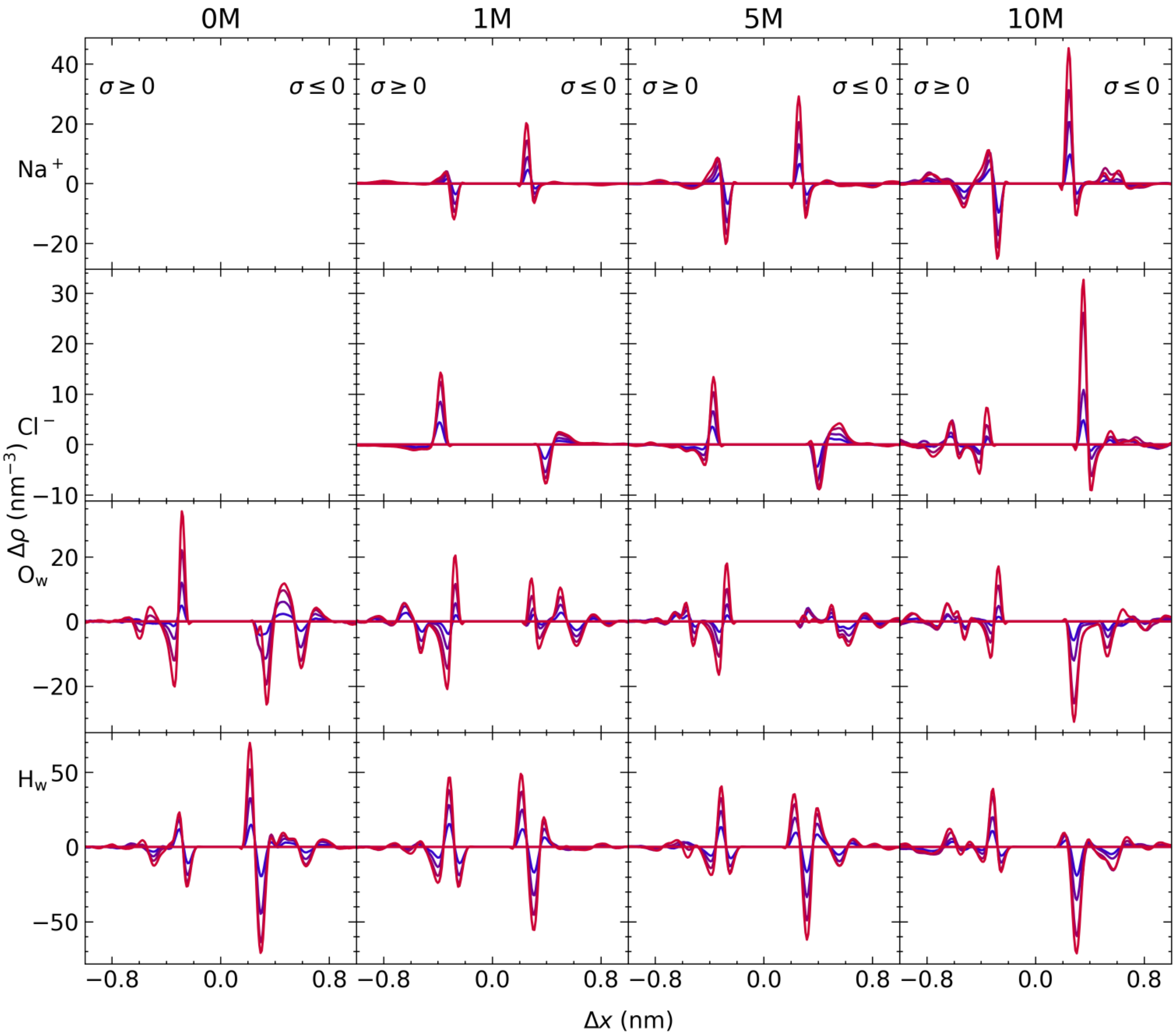


Figure S5: Change in the atom densities ($\Delta\rho$) as a function of distance from the graphite electrode according to the applied surface charge density ($|\sigma| = 0 \rightarrow 0.77\ e\ \mathrm{nm}^{-2}$ as indicated by the blue→red colour scale). Atom types are provided on the left, and target bulk concentrations are indicated the top of the grid.

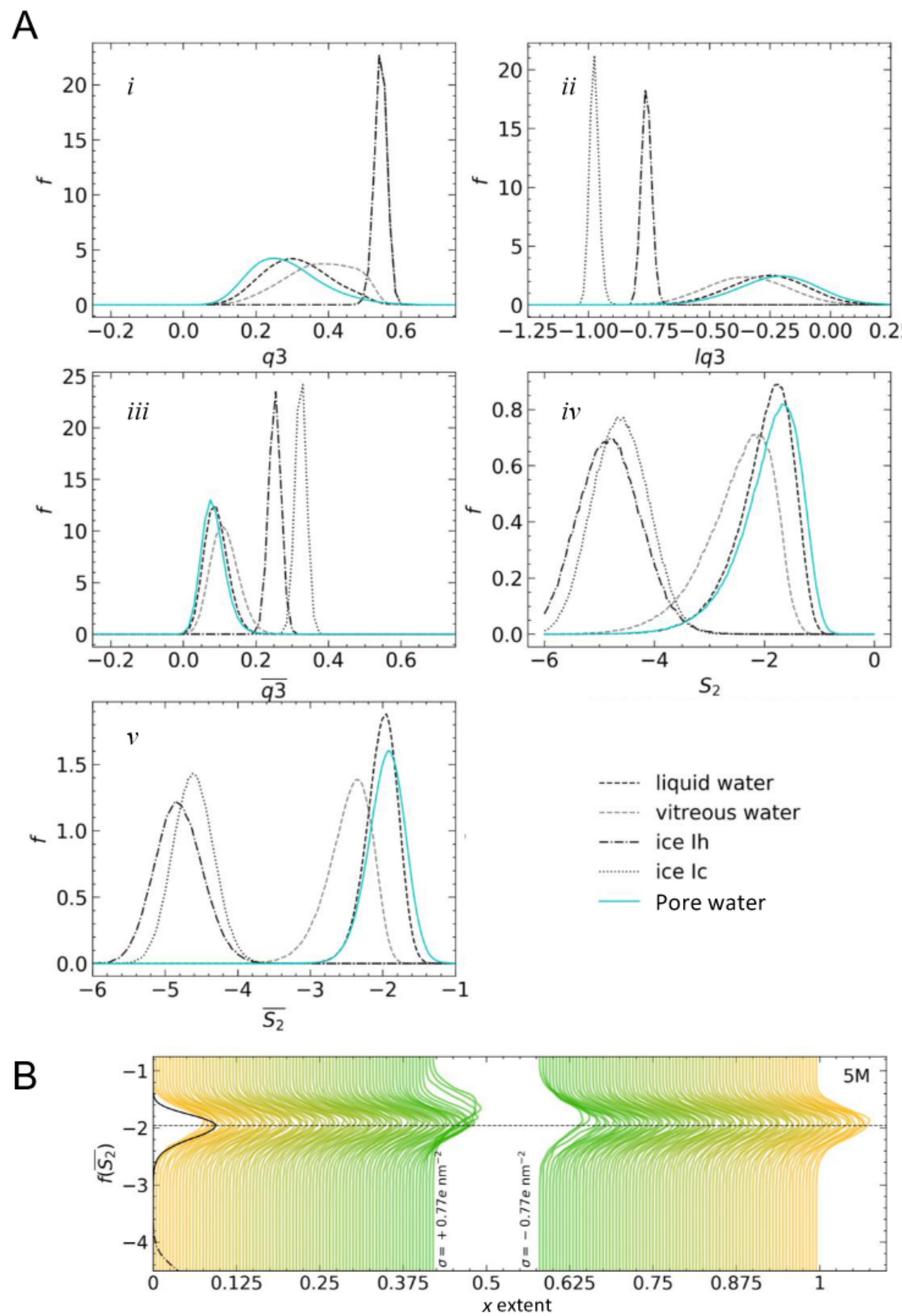


Figure S6: A) Order parameter analysis for water in C$\mu$MD simulations of 5 M NaCl(aq) at charged graphite with surface charge density, $|\sigma| = 0.77\,e$ nm$^{-2}$. The probability density for $q3$ ($i$), local q3 ($ii; lq3$), local average q3 ($iii; \overline{q3}$), approximate pair entropy ($iv; S_2$) and local average approximate pair entropy ($v; \overline{S_2}$) are provided. The distributions for water in bulk liquid, vitreous (liquid water crash cooled to 100 K), hexagonal ice (ice $I_h$) and cubic ice ($I_c$) are also provided. B) Probability densities for $\overline{S_2}$ in slices of the cell $x$ axis. The bulk liquid water and ice $I_h$ distributions are provided on the $y$-axis.

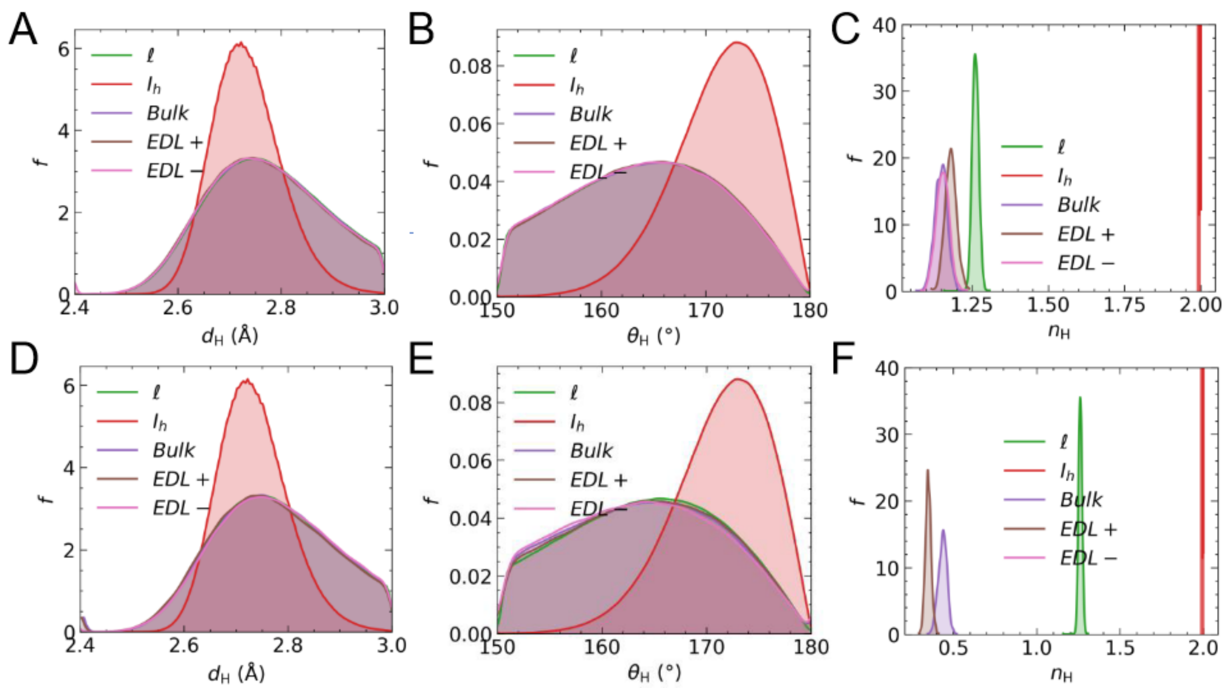


Figure S7: H-bonds for bulk liquid water ($\ell$), ice $I_h$, and water in the bulk and EDL regions of C$\mu$MD simulations of graphite in contact with NaCl(aq) where the surface charge density was $|\sigma| = 0.77\,e$ nm$^{-2}$. $d_H$ and $\theta_H$ refer to the H-bond D—H$\cdots$A distance (A and D) and angle (B and E), respectively, where D, H and A refer to the oxygen donor, bonded hydrogen and oxygen acceptor, respectively. The number of H-bond donors per water molecule is provided in C, and F. A-C are for cases where the concentration was 0 M, while D-E provide the results from simulations at 10 M.

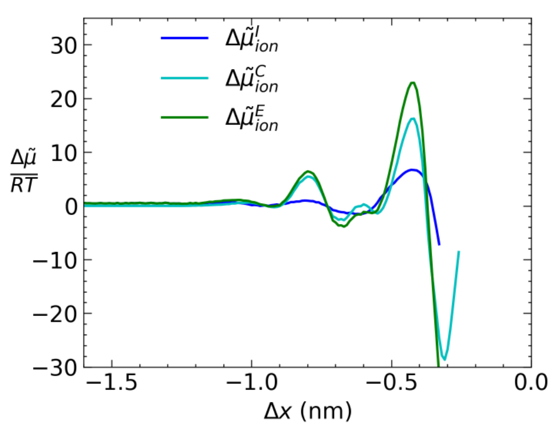


Figure S8: Contributions to the electrochemical potential of ions ($\Delta\tilde{\mu}$) in solution at graphite with $\sigma = +0.77$ $e$ nm$^{-2}$. $\Delta\tilde{\mu}^{I} = RT\left[\ln m_{Na}(x) m_{Cl}(x)\right]$; $\Delta\tilde{\mu}^{C} = (2\omega - 1)F\psi(x)$; and, $\Delta\tilde{\mu}^{E} = RT\ln\left[\gamma_{ion}(m_{Na}(x))\gamma_{ion}(m_{Cl}(x))\right]$.

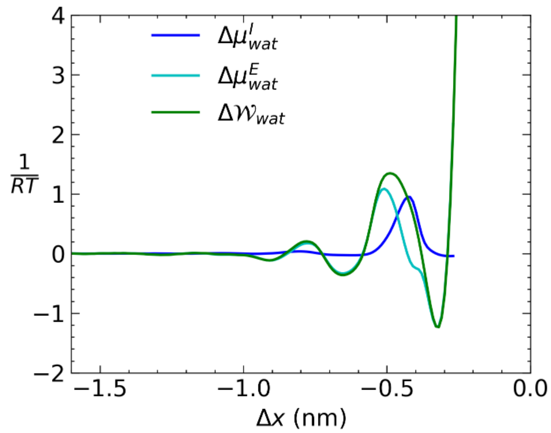


Figure S9: Contributions to ($\Delta\mathcal{W}_{wat}(x)$) in 1 M NaCl(aq) solution at graphite with $\sigma = +0.77e$ nm$^{-2}$. See equation 14 in the main paper for details.

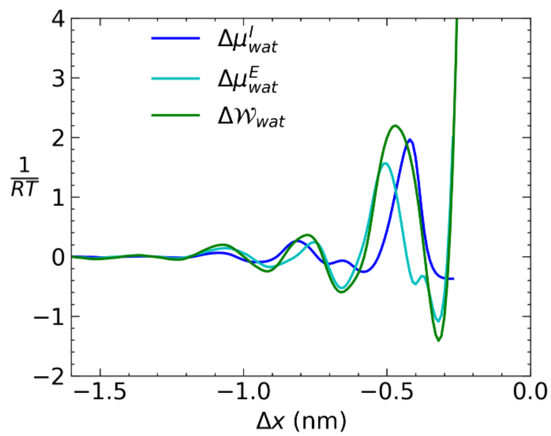


Figure S10: Contributions to ($\Delta\mathcal{W}_{wat}(x)$) in 10 M NaCl(aq) solution at graphite with $\sigma = +0.77e$ nm$^{-2}$. See equation 14 in the main paper for details.